

## Articles

---

### Characterization of a Bacterial $\beta$ -1,3-Galactosyltransferase with Application in the Synthesis of Tumor-Associated T-Antigen Mimics<sup>†</sup>

Wen Yi,<sup>‡,||</sup> Ramu Sridhar Perali,<sup>§</sup> Hironobu Eguchi,<sup>‡</sup> Edwin Motari,<sup>§</sup> Robert Woodward,<sup>§</sup> and Peng George Wang<sup>\*,‡,§,||</sup>

*Department of Biochemistry, Department of Chemistry, and The Ohio State Biochemistry Program, The Ohio State University, Columbus, Ohio 43210*

*Received October 15, 2007; Revised Manuscript Received November 14, 2007*

**ABSTRACT:** T-Antigen (Gal- $\beta$ 1,3-GalNAc- $\alpha$ -O-Ser/Thr) is an important precursor of mucin-type O-glycans. T-Antigen is found to be closely associated with cancer progression and metastasis and has been used to develop carbohydrate-based anticancer vaccines. Enzymatic synthesis of T-antigen disaccharides have relied on the use of  $\beta$ -1,3-galactosyltransferases recently cloned and characterized from several eukaryotic organisms. However, its application is limited by the difficulty of obtaining homogeneous enzymes and the strict substrate specificity of enzymes. Recently, a number of bacteria have been found to express carbohydrate structures that mimic host glycans. The corresponding glycosyltransferases have been exploited in the facile synthesis of a number of clinically important glycoconjugate mimics. In this study, we biochemically characterized a bacterial  $\beta$ -1,3-galactosyltransferase (WbiP) from *Escherichia coli* O127, which expresses a T-antigen mimic in the lipopolysaccharide (LPS) structure. Substrate study showed that WbiP could readily glycosylate a series of *N*-acetylgalactosamine (GalNAc) analogues with  $\alpha$ -substitutions at the reducing end, including glycosylated Ser and Thr (GalNAc- $\alpha$ -O-Ser/Thr), which illustrates the use of WbiP for the facile synthesis of T-antigens. Alignment of a group of putative bacterial  $\beta$ -1,3-galactosyltransferases revealed the presence of two conserved DXD motifs, possibly suggesting a different functional role of each motif. Site-directed mutagenesis, enzyme kinetics as well as UDP-bead binding assays were carried out to investigate the role of each DXD motif in WbiP. The results suggest that <sup>88</sup>DSD<sup>90</sup> is critical in the binding of sugar donor UDP-Gal, whereas <sup>174</sup>DYD<sup>176</sup> may participate in the binding of the sugar acceptor. This study expands the scope of using bacterial glycosyltransferases as tools for *in vitro* synthesis of glycoconjugate mimics with clinical significance.

Mucin-type O-linked glycosylation is a ubiquitous protein post-translational modification in higher eukaryotes and is

involved in a number of fundamental biological processes (1). For example, mucin-type O-glycans can protect proteins from proteolytic degradation (2), regulate the serum half-life of chemokines *in vivo* (3, 4), modulate the intracellular trafficking of proteins (5), mediate cell adhesion events such as sperm-egg fertilization (6), microbe-host interaction, and viral infection (7), and serve as tumor-associated antigens (8).

Mucin-type O-glycan is initiated with an  $\alpha$ -*N*-acetylgalactosamine (GalNAc<sup>1</sup>) attached to the hydroxyl group of

<sup>†</sup> P. G. Wang acknowledges support from an endowed Ohio Eminent Scholar Professorship on Macromolecular Structure and Function in the Department of Biochemistry at The Ohio State University.

\* To whom correspondence should be addressed. Phone: (614) 292-9884. Fax: (614) 688-3106. E-mail: wang.892@osu.edu.

<sup>‡</sup> Department of Biochemistry.

<sup>§</sup> Department of Chemistry.

<sup>||</sup> The Ohio State Biochemistry Program.

Ser/Thr side chains and elaborated by Golgi-resident glycosyltransferases to generate a series of core structures (1). Core-1 structure (also called T-antigen, Gal- $\beta$ 1,3-GalNAc- $\alpha$ -O-Ser/Thr) is the precursor of surface antigens in human epithelial and blood group cells (9). T-Antigens are masked in normal tissues but uncovered during malignancy (10). Previous research has shown that T-antigens are expressed in >90% of primary human carcinomas, and high expression levels of T-antigens are correlated with increased metastasis and aggressiveness of several types of cancers (11, 12). Therefore, T-antigens have been used in clinical trials to develop carbohydrate-based cancer vaccines.

Various mucosal pathogens express carbohydrate structures on their cell surface that mimic host structures as a means of evading immune clearance. For example, *Haemophilus influenzae* is a pathogen that routinely colonizes the upper respiratory tract. It is often associated with serious infectious diseases such as meningitis, septicemia, and emphysema. *H. influenzae* strain Rd express a lipooligosaccharide, globotetraose (13), on its cell surface that can mimic host glycolipids, which is important for the pathogenesis of diseases. *Campylobacter jejuni* has been recognized as a major cause of acute gastroenteritis in humans. One of the most common strains associated with the development of Guillain-Barre syndrome, *C. jejuni* O:19 has been shown to display molecular mimicry of gangliosides (GM1, GD1a, GD3, and GT1a) (14). Another common gastric pathogen, *Helicobacter pylori*, expresses histo blood group antigens, most of which are type II glycoconjugate antigens, Lewis X (Le<sup>x</sup>) and Lewis Y (Le<sup>y</sup>) (15–17). The expression of Lewis antigens by *H. pylori* has also been suggested to play a role in the pathogenesis of chronic type B gastritis and gastric and duodenal ulcers.

*E. coli* O127 belongs to the O serogroup of enteropathogenic *Escherichia coli* (EPEC) strains, which are important causes of infantile diarrhea in developing countries (18–20). *E. coli* O127 strains have been isolated from children with diarrhea worldwide. In addition, *E. coli* O127 was reported to possess high human blood group H (O) activity. The elucidation of the chemical structure of the cell surface O-antigen (21) confirmed that *E. coli* O127 expressed mimicry of human blood group H antigen (Figure 1). The O-antigen biosynthetic gene cluster (GenBank Accession no. AY493508) contains multiple genes needed for the assembly of *E. coli* O127 polysaccharide structures. Among them, three genes (*orf3*, *orf12*, and *orf13*) encode putative glycosyltransferases involved in the synthesis of repeating oligosaccharide units. *Orf12* (WbiP) contains a conserved domain found in glycosyltransferase family 2. It shows 59% protein sequence identity and 82% similarity to WbnJ from *E. coli* O86, which was previously characterized as a  $\beta$ -1,3-galactosyltransferase (22). Thus we propose that WbiP encodes a  $\beta$ 1,3-galactosyltransferase that makes the Gal- $\beta$ 1,3-GalNAc moiety (T-antigen mimicry) present in the repeating unit structure. In

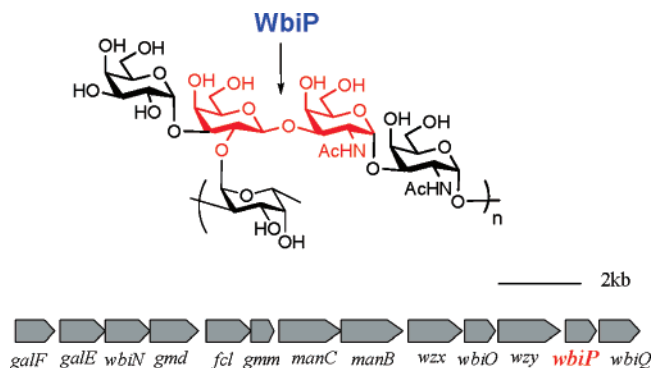


FIGURE 1: O-polysaccharide structure of *E. coli* O127 and its biosynthetic gene cluster. (T-Antigen mimic structure catalyzed by WbiP is highlighted.)

this study, we present a detailed biochemical characterization of WbiP and a series of mutants. Moreover, we show that this bacterial  $\beta$ -1,3-galactosyltransferase is implicated in the facile synthesis of T-antigen mimics.

## MATERIALS AND METHODS

**Bacterial Strains, Plasmids, and Materials.** *E. coli* O127: K63(B8) was obtained from American Type Culture Collection (Rockville, MD). *E. coli* competent cell DH5 $\alpha$  [*lacZ* $\Delta$ M15 *hsdR* *recA*] was from Gibco-BRL Life Technology. *E. coli* competent cell BL21 (DE3) [F *ompT* *hsdS*<sub>B</sub> (*r<sub>BMB</sub>*) *gal* *dcm* (DE3)] were from Novagen Inc. (Madison, WI). Expression plasmid pET28a was purchased from Novagen (Carlsbad, CA). HiTrap Chelating Ni HP column was obtained from GE Healthcare (Piscataway, NJ). All other chemicals and solvents were from Sigma-Aldrich.

**Cloning, Expression, and Purification of WbiP.** The *wbiP* gene was amplified by PCR from the *E. coli* O127 chromosome. The primers with restriction sites underlined for amplification of each gene were as follows:

Forward: 5' GAGATATACATATGAAAAATGTTG-GTTTTATTG (*Nde*I); Reverse: 5' CCGCCTCGAGTCAAC-CTAAAATAATGCTTTTATATG (*Xho*I). The DNA fragments obtained were digested with corresponding restriction enzymes and inserted into pET28a vector linearized by the same restriction enzymes to form pET28a-*wbiP* recombinant plasmid. The recombinant plasmid was confirmed by restriction mapping and sequencing. The correct constructs were subsequently transformed into *E. coli* BL21 (DE3) for protein expression. *E. coli* BL21 (DE3) harboring the recombinant plasmid was grown at 37 °C in 1 L of Luria-Bertani (LB) medium with 35  $\mu$ g/mL kanamycin antibiotic. When the cells were grown to OD 0.5–0.7, isopropyl 1-thio- $\beta$ -D-galactopyranoside (IPTG) was added to a final concentration of 0.4 mM. Expression was allowed to proceed for 12 h at 25 °C. Cells were harvested, washed with 20 mM Tris-HCl (pH = 7.0) and stored at –80 °C until needed. In protein purification, the cell pellet was resuspended in buffer (20 mM Tris-HCl, pH 7.5, 0.5 M NaCl, 5 mM imidazole, 1 mM PMSF) and disrupted by brief sonication (Branson Sonifier 450, VWR Scientific) on ice. The lysate was cleared by centrifugation (15 000g, 20 min, 4 °C) and loaded at a low rate of 3 mL/min onto a 5 mL Ni<sup>2+</sup>-NTA chelating column equilibrated with 20 mM Tris-HCl, pH 7.5, 0.5 M NaCl, and 5 mM imidazole. The column was washed with 10

<sup>1</sup> Abbreviations: ESI-MS, electrospray ionization mass spectrometry; Gal, galactose; GalNAc, N-acetylgalactosamine; HPLC, high performance liquid chromatography; MALDI-MS, matrix-assisted laser desorption/ionization-mass spectrometry; NMR, nuclear magnetic resonance; SDS-PAGE, sodium dodecyl sulfate-polyacrylamide gel electrophoresis; Ser, serine; Thr, threonine; TLC, thin layer chromatography; UDP-Gal, uridine 5'-diphospho-galactose; UDP-GalNAc, uridine 5'-diphospho-N-acetylgalactosamine; UDP-Glc, uridine 5'-diphospho-glucose; GDP-Fuc, guanosine 5'-diphospho-fucose.

column volumes of 50 mM imidazole in the same buffer, and the protein was eluted with 250 mM imidazole, followed by analysis using SDS-PAGE.

**Radioactive Enzymatic Assay.** Protein concentration was determined by Bradford method. One unit of enzyme activity was defined as the amount of enzyme required to transform 1  $\mu$ mol of sugar donor to acceptor per minute at 37 °C. Enzyme assays were performed at 37 °C for 2 h in a final volume of 100  $\mu$ L containing 20 mM Tris-HCl, pH 7.0, 10 mM MnCl<sub>2</sub>, 0.3 mM radioactively labeled UDP-D-[6-<sup>3</sup>H]-galactose (specific activity: 4.3 Ci/mmol) as sugar donor, 10 mM monosaccharide *N*-acetylgalactosamine (GalNAc) as sugar acceptor, and variable amount of enzymes. Acceptor was omitted as the blank control. The reaction was terminated by adding 100  $\mu$ L of ice cold 0.1M EDTA. Dowex 1  $\times$  8-200 chloride anion exchange resin was then added in a water suspension (0.8 mL, v/v = 1/1). After centrifugation, supernatant was collected in a 20 mL plastic vial and ScintiVerse BD (10 mL) was added. The vial was vortexed thoroughly before the radioactivity of the mixture was measured in a liquid scintillation counter (Beckmann LS-3801 counter).

**Enzyme Assay with HPLC and MALDI-MS.** To a tube containing 0.05 mg of GalNAc were added 10  $\mu$ L of 0.1 M Tris-HCl, pH 7.5, 5  $\mu$ L of 0.1 M MnCl<sub>2</sub>, 5  $\mu$ L of 50 mM UDP-Gal, and 0.02 mg of WbiP (20  $\mu$ L). The reaction was run at room temperature for 1 h and quenched by addition of 50  $\mu$ L of cold methanol. The mixture was centrifuged to remove the precipitated proteins. The supernatant was evaporated to dryness. The mixture was then labeled with 2-aminobenzamide (2-AB) as described. Postlabeling cleanup was done by applying the labeling sample onto a Whatman 3MM chromatography paper and performing ascending chromatography in acetonitrile for 2 h. The labeling product was eluted from the paper with 0.5 mL of H<sub>2</sub>O and further separated on a normal phase analytic HPLC column as described. The peaks were detected with a fluorescence detector ( $\lambda_{\text{ex}}$  = 330 nm,  $\lambda_{\text{em}}$  = 420 nm) and collected and characterized with MALDI-MS.

**Site-Directed Mutagenesis of WbiP.** QuikChange Site-Directed Mutagenesis Kit (Stratagene) was used to construct all the mutants from the parent plasmid, pET28a-WbiP, using the primers shown in the Supporting Information Table S1. Expression, purification, and enzyme activity assay were carried out following the abovementioned procedures.

**Kinetic Studies of Wild-Type and Mutants.** Reactions were performed at 37 °C for 40 min in a reaction buffer containing 20 mM Tris-HCl (pH 7.5), 10 mM MnCl<sub>2</sub>, 0.3 mM UDP-D-[6-<sup>3</sup>H]-Gal and 20  $\mu$ g of enzyme. To determine apparent  $K_m$  values, the concentration of GalNAc was varied as follows: 10 mM, 20 mM, 40 mM, and 80 mM. To determine the  $K_m$  value for UDP-Gal, 3  $\mu$ M of UDP-D-[6-<sup>3</sup>H]-Gal was supplemented with different amounts of cold UDP-Gal to achieve varying final concentrations (0.08, 0.1, 0.3, and 0.6 mM), with a fixed GalNAc concentration at 20 mM. The parameters  $K_m$  and  $V_{\text{max}}$  were obtained by Lineweaver-Burk plots of substrate concentration-initial velocity.

**Enzymatic Synthesis of T-Antigen Mimics and Structural Characterization.** A one-pot reaction was conducted for 2 days at room temperature in a final volume of 1.0 mL containing 20 mM Tris-HCl (pH 7.5), 10 mM MnCl<sub>2</sub>, 10 mM UDP-Gal, 15 mM acceptor GalNAc-OMe, and 20  $\mu$ g

of WbiP. The progress of the reaction was monitored by thin-layer chromatography [i-PrOH/H<sub>2</sub>O/NH<sub>4</sub>OH = 8:2:2 (v/v/v)] conducted on Baker Si250F silica gel TLC plates. Products were visualized by staining solution (anisaldehyde/MeOH/H<sub>2</sub>SO<sub>4</sub> = 1:15:2 (v/v/v)). After complete conversion of donor substrate, protein was removed by brief boiling and centrifugation (12 000g, 5 min). The supernatant mixture was purified by gel filtration chromatography Bio-Gel P2 (Bio-Rad, CA). The desired fractions were pooled, lyophilized, and stored at -20 °C.

Mass spectra (ESI) were run in the negative mode at the mass spectrometry facility at the Ohio State University. Product structure was identified by <sup>1</sup>H and <sup>13</sup>C NMR spectroscopy using a 500-MHz Varian VXR500 NMR spectrometer. Product structure was identified through one-dimensional (selective COSY, relay COSY, and NOE) and two-dimensional (COSY, HMQC, NOESY, and HMBC) <sup>1</sup>H/<sup>13</sup>C NMR. The oligosaccharide product was repeatedly dissolved in D<sub>2</sub>O and lyophilized before NMR spectra were recorded at 303 K in a 5 mm tube. <sup>1</sup>H NMR (500 MHz, D<sub>2</sub>O): 1.98 (s, 3H), 3.35 (s, 3H), 3.47 (dd, 1H,  $J$  = 9.9 Hz,  $J$  = 7.8 Hz), 3.57 (dd, 1H,  $J$  = 9.9 Hz,  $J$  = 3.4 Hz), 3.61 (dd, 1H,  $J$  = 7.7 Hz,  $J$  = 4.6 Hz), 3.71 (m, 2H), 3.72 (m, 2H), 3.86 (d, 1H,  $J$  = 3.3 Hz), 3.91 (dd, 1H,  $J$  = 7.3 Hz,  $J$  = 5.0 Hz), 3.96 (dd, 1H,  $J$  = 11.1 Hz,  $J$  = 3.1 Hz), 4.18 (d, 1H,  $J$  = 2.9 Hz), 4.29 (dd, 1H,  $J$  = 11.1 Hz,  $J$  = 3.7 Hz), 4.41 (d, 1H,  $J$  = 7.8 Hz), 4.74 (d, 1H,  $J$  = 3.7 Hz).  $\delta$  <sup>13</sup>C NMR (125 MHz, D<sub>2</sub>O):  $\delta$  175.0, 105.1, 98.7, 77.7, 75.3, 72.9, 71.0, 70.8, 69.1, 69.0, 61.6, 61.3, 55.5, 49.0, 22.4. HRMS,  $m/z$ : Calculated C<sub>15</sub>H<sub>27</sub>NO<sub>11</sub> + Na: 420.1476; found: 420.1474.

**UDP-Binding Assay.** A 30  $\mu$ L aliquot of fresh UDP-beads (CalBiochem) was washed three times with binding buffer (20 mM Tris-HCl pH 7.0, 0.1 M NaCl, 5.0 mM MgCl<sub>2</sub>). The beads were incubated on a roller at 4 °C for 1 h with 40  $\mu$ L of purified recombinant wild type WbiP and its variant mutants (50  $\mu$ g of proteins) in binding buffer. The negative control involved incubation of wild type WbiP with 10 mM UDP to inhibit binding to UDP-beads. The beads were harvested by centrifugation for 1 min at 1000g, followed by washing with binding buffer three times. The bound proteins were treated in SDS loading buffer at 100 °C for 5 min before analysis by SDS-PAGE and western blotting with anti-His antibody.

## RESULTS

**Expression, Purification, and Enzymatic Assay of WbiP Protein.** The full open reading frame of *wbiP* gene (750 bp) was amplified from *E. coli* O127 genomic DNA and subsequently cloned into pET-28a vector. The recombinant plasmid was transformed into *E. coli* BL21(DE3) strain for induced expression with 0.4 mM IPTG at 25 °C. WbiP protein has an apparent molecular weight of 28 kDa estimated by SDS-PAGE (data not shown), similar to the theoretical value (28.6 kDa) calculated from its predicted amino acid sequence. Primary sequence analysis shows that WbiP has no transmembrane segments, consistent with the result that we were able to purify WbiP without difficulty even though detergents were omitted.

To investigate the function of WbiP, we tested a panel of radiolabeled sugar donors (UDP-Gal, UDP-GalNAc, GDP-



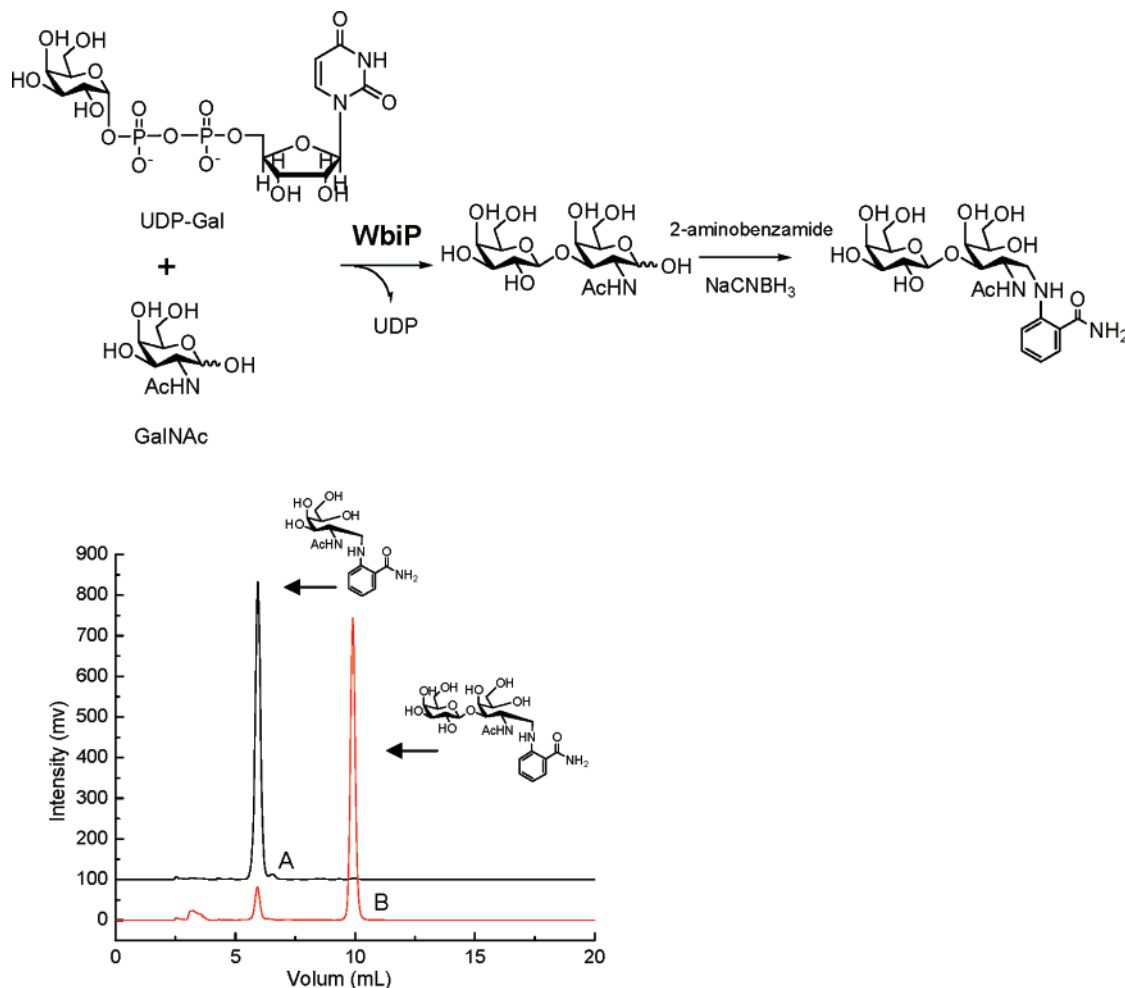


FIGURE 2: WbiP-catalyzed reaction and HPLC identification of product.

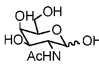
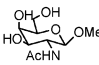
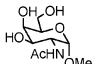
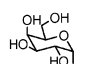
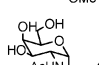
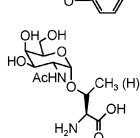
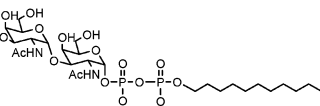
Fuc, and UDP-Glc) with GalNAc as an acceptor. The results showed that WbiP displayed high activity with UDP-Gal as the sugar donor, nearly 10 fold reduced efficiency with UDP-GalNAc (see Supporting Information, Figure S1), and no activity with GDP-Fuc and UDP-Glc. Thus, the donor specificity demonstrated that *wbiP* encodes a galactosyltransferase, consistent with the bioinformatics analysis. To confirm the galactosyltransferase activity of WbiP, we set up a 50  $\mu$ L scale reaction, which contained 0.05 mg of GalNAc, 5  $\mu$ L of 50 mM cold UDP-Gal, and 0.02 mg of WbiP (20  $\mu$ L). The reaction product was then labeled with 2-aminobenzamide (2-AB) and analyzed via a normal phase analytical HPLC columns. The molecular weight was characterized by MALDI-MS. The 2-AB-labeled starting material GalNAc has a retention volume of 6 mL. When the labeled product of the reaction was analyzed, a new peak with a retention volume of 10 mL was observed (Figure 2). When this peak was collected and subjected to MALDI-MS analysis, a  $m/z$  ratio of 526.20  $[M + Na]^+$  was observed (see Supporting Information), consistent with a 2-AB-labeled Gal-GalNAc disaccharide. Therefore, the results from both the radioactive assay and the HPLC/MS assay confirm that WbiP encodes a galactosyltransferase.

**Characterization of Linkage Specificity and Enzymatic Synthesis of T-Antigen Mimics.** To confirm that WbiP catalyzes the formation of the  $\beta$ -1,3-linkage, a reaction was carried out with GalNAc- $\alpha$ -OMe as an acceptor. GalNAc-

$\alpha$ -OMe was used instead of GalNAc because GalNAc- $\alpha$ -OMe has the same reactivity as GalNAc (see below) while the fixed configuration of the anomeric carbon by OMe substitution facilitates the NMR analysis. A milligram scale reaction was conducted using 8 mg of GalNAc- $\alpha$ -OMe and 1.5 equiv of UDP-Gal. The reaction was incubated at room temperature overnight and monitored by TLC. The disaccharide product was isolated by gel filtration chromatography. A total of 11 mg of disaccharide (85% yield) was collected to allow structural analysis by NMR spectroscopy.

**Substrate Specificity of WbiP.** Purified WbiP was used to investigate its specificity toward various sugar acceptors (Table 1). The results indicate that the  $\alpha$ -configuration at the reducing end of GalNAc is important for enzyme activity since changing the configuration from  $\alpha$  to  $\beta$  makes GalNAc a poor substrate for WbiP (GalNAc- $\beta$ -OMe has only 15% activity compared to GalNAc- $\alpha$ -OMe). The *N*-acetyl at C2 of GalNAc is essential for enzyme recognition, since no detectable activity was observed when Gal- $\alpha$ -OMe was used as an acceptor. Furthermore, WbiP can tolerate substitution on the 1-O position of GalNAc, demonstrated by observation that a series of  $\alpha$ -substitutions ( $\alpha$ -OMe,  $\alpha$ -OBn,  $\alpha$ -O-Ser/Thr, and  $\alpha$ 1,3-GalNAc-PP-C<sub>11</sub>) have comparable reactivities. It is worth noting that GalNAc- $\alpha$ -O-Ser/Thr are the biosynthetic precursors for T-antigens of mucin-type O-glycans. The fact that these two glycosylated amino acids serve as good substrates indicates that WbiP can be potentially used

Table 1: Substrate Specificity of WbiP

| Acceptors   |   | Relative activity % |
|---|---|---------------------|
|  | (GalNAc)  | 100                 |
|  | (GalNAc- $\beta$ -OMe)  | 15                  |
|  | (GalNAc- $\alpha$ -OMe)                                       | 105                 |
|  | (Gal- $\alpha$ -OMe)  | N/A                 |
|  | (GalNAc- $\alpha$ -OPh)                                       | 92                  |
|  | (GalNAc- $\alpha$ -O-Thr(Ser))                                | 95                  |
|  | (GalNAc- $\alpha$ -1,3-GalNAc- $\alpha$ -PP-C <sub>11</sub> ) | 85                  |

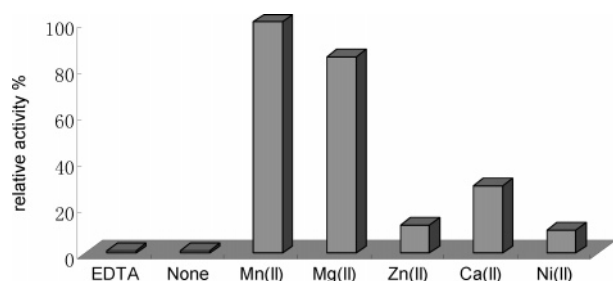


FIGURE 3: Metal ion requirement of WbiP. The concentration of EDTA and metal ions are all at 10 mM.

for the large scale synthesis of T-antigens for biomedical studies. Not surprisingly, WbiP readily accepts  $\alpha$ -GalNAc- $\alpha$ 1,3-GalNAc-PP-C<sub>11</sub> as a substrate, which is an analogue of the immediate synthetic substrate of WbiP based on the *E. coli* O127 O-repeating unit structure. Thus taken together, the acceptor pattern shown in the assay is in agreement with the proposed function of WbiP in the biosynthesis of the *E. coli* O127 O-repeating unit.

**Determination of Metal Ion Effect on WbiP.** Many glycosyltransferases are found to contain a short conserved amino acid sequence called the DXD motif and exhibit a requirement for a divalent metal cation for activity. Sequence analysis shows that WbiP contains two DXD motifs (<sup>88</sup>DSD<sup>90</sup> and <sup>174</sup>DYD<sup>176</sup>), suggesting that WbiP activity requires a metal ion cofactor. To further investigate the metal ion requirements, various divalent metal cations as well as EDTA were incubated in a series of separate reactions. As predicted, WbiP activity requires metal ions with Mn<sup>2+</sup> and Mg<sup>2+</sup> as the preferred cations (Figure 3). The activity was completely abolished in the absence of metal ions or in the presence of 10 mM EDTA. Thus WbiP belongs to glycosyltransferase superfamily A (GTA), in which the DXD motif plays a role in coordinating the binding of sugar nucleotide donors in the active site.

**Site-Directed Mutagenesis Study of DXD Motifs and Enzyme Kinetics of WbiP and Its Mutants.** Sequence alignment of a group of bacterial  $\beta$ 1,3-galactosyltransferases (putative and characterized) shows that they all possess two DXD or DXD-like motifs (Figure 4), suggesting this might reflect a common catalytic mechanism in these galactosyltransferases. In order to investigate the functional role of each DXD motif, we mutated the aspartic acid residues of the DXD motifs in the WbiP sequence. Aspartic acid residues in each DXD motif were mutated to alanine and glutamic acid, respectively. A total of eight mutations were generated: D88A, D88E, D90A, D90E, D174A, D174E, D176A, and D176E. The mutagenic primer pairs are listed in Supporting Information. WbiP mutants were expressed at a similar level compared to the wild-type (data not shown), suggesting that the mutations in the DXD motifs do not compromise protein folding and stability. The enzyme activity of each mutant was assessed using the radioactive assay. The result (Figure 5) shows that mutating aspartic acid to alanine at <sup>88</sup>DSD<sup>90</sup> completely abolishes the enzyme activity, while the same mutation at <sup>174</sup>DYD<sup>176</sup> still retains some marginal activity (12% and 10% for D174A and D176A, respectively). This observation indicates that <sup>88</sup>DSD<sup>90</sup> may play a more essential role in catalysis than <sup>174</sup>DYD<sup>176</sup>. The change of aspartic acid residue to its conserved counterpart, glutamic acid, in <sup>88</sup>DSD<sup>90</sup> partially restored enzyme activity (8% for D88E and 10% for D90E), indicating the importance of charge in these positions for catalysis. The same mutations at <sup>174</sup>DYD<sup>176</sup> restored enzyme activity to a higher level (23% for D174E and 31% for D176E), further confirming that the requirement of aspartic acid residues in this position is less stringent.

Kinetic parameters (Table 2) were determined for both the wild-type and mutant enzymes. The wild-type enzyme has apparent *K<sub>m</sub>* values of 31  $\mu$ M and 16.1 mM for donor UDP-Gal and acceptor GalNAc, respectively. These are

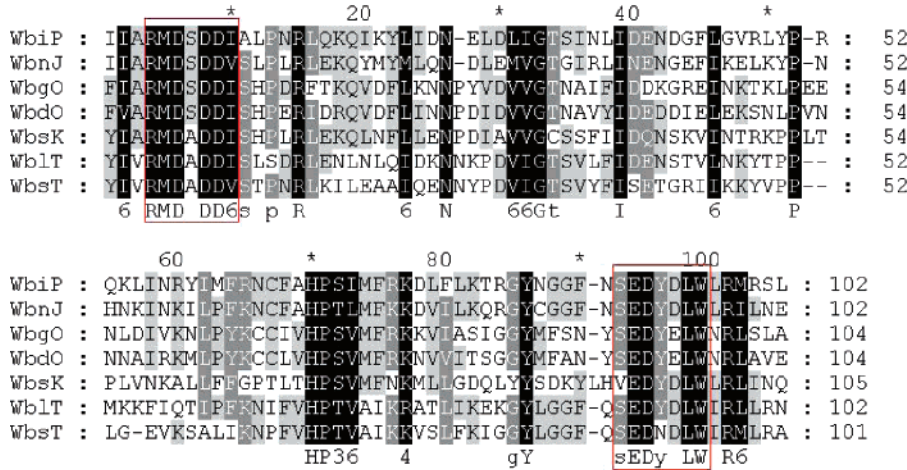


FIGURE 4: Amino acid sequence alignment of segments from different  $\beta$ 1,3-galactosyltransferases. (Conserved DXD motifs are bracketed with red.) WbiP: from *E. coli* O127O127:K63(B8), AAR90893; WbnJ: from *E. coli* O86:H2, AAV80758; WbgO: from *E. coli* O55:H7, AAL67559; WbdO: from *Salmonella enterica* subsp. *salamae* serovar Greenside 50, AAV34525; WbsK: *E. coli* O128:B12, AAO37699; WblT: from *Photobacterium luminescens* subsp. *laumondii* TTO1, CAE17191; WbsT: from *E. coli* O126, DQ465248.

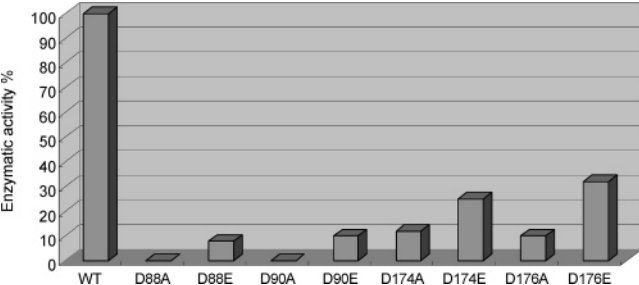


FIGURE 5: Enzymatic activity of WbiP mutants.

Table 2: Kinetic Parameters of WbiP and Mutants

| WbiP  | UDP-Gal                   |                      |  | GalNAc                    |               |                                       |
|-------|---------------------------|----------------------|--|---------------------------|---------------|---------------------------------------|
|       | $K_{cat}$<br>( $s^{-1}$ ) | $K_m$<br>( $\mu M$ ) | $K_{cat}/K_m$<br>( $s^{-1} \mu M^{-1}$ ) | $K_{cat}$<br>( $s^{-1}$ ) | $K_m$<br>(mM) | $K_{cat}/K_m$<br>( $s^{-1} mM^{-1}$ ) |
| WT    | 11.2                      | 31                   | 0.36                                     | 15.3                      | 16.1          | 0.95                                  |
| D88E  | 0.08                      | 232                  | 0.00034                                  | 2.2                       | 25.2          | 0.087                                 |
| D90E  | 0.2                       | 251                  | 0.00079                                  | 0.6                       | 32.3          | 0.018                                 |
| D174A | 2.9                       | 58                   | 0.05                                     | 0.4                       | 375           | 0.0011                                |
| D174E | 3.7                       | 47                   | 0.079                                    | 1.7                       | 175           | 0.0097                                |
| D176A | 1.0                       | 67                   | 0.015                                    | 1.2                       | 237           | 0.0051                                |
| D176E | 3.9                       | 43                   | 0.091                                    | 5.1                       | 140           | 0.036                                 |

similar to the values obtained in other well-characterized glycosyltransferases. Notably, D88E and D90E mutants have considerably higher  $K_m$  values for UDP-Gal but quite similar  $K_m$  values for GalNAc. On the contrary, mutations in D174 and D176 resulted in higher  $K_m$  values for GalNAc but similar values for UDP-Gal. This observation suggests that <sup>88</sup>DSD<sup>90</sup> is critical in the binding of sugar donor UDP-Gal, while <sup>174</sup>DYD<sup>176</sup> may participate in the binding of the sugar acceptor. These two DXD motifs thus have different functional roles in catalysis.

**UDP-Beads Binding Assay.** To further investigate the involvement of the <sup>88</sup>DSD<sup>90</sup> motif in the binding of the sugar donor, we carried out a UDP-beads binding assay with purified wild-type and mutant enzymes (Figure 6). Wild-type WbiP binds efficiently to UDP-beads. The binding was substantially decreased in the presence of 10 mM UDP, indicating that the binding of WbiP to the beads is specific. D174A and D176A mutants have similar binding efficiency as compared to the wild-type. On the other hand, D88A and

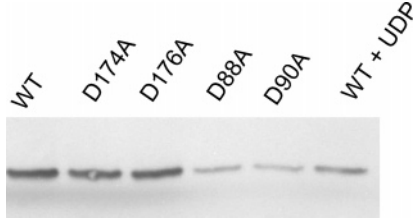


FIGURE 6: UDP-beads binding assay.

D90A mutants have remarkably reduced binding, suggesting that D88 and D90 are involved in the binding of sugar donor UDP-Gal. These results are consistent with the kinetic studies.

## DISCUSSION

Cell surface glycoconjugates contain rich structural information that is central in virtually every aspect of biological processes, ranging from protein folding, cellular development, and host–pathogen interaction to immune regulation (23). In recent years, the study of the structure–function relationship of glycoconjugates has been aided tremendously by the *in vitro* synthesis of structurally defined glycoconjugates and their analogues. Chemical glycosylation, well documented for its synthetic flexibility, has been successful in preparing a wide range of carbohydrate structures. However, the chemical approach still suffers from tedious protection/deprotection steps and difficult purification of products. On the other hand, with the rapid development of genomic sequencing, a growing number of glycosyltransferases have been characterized with a wide spectrum of acceptor specificity that has proven invaluable for the facile synthesis of a variety of glycoconjugate structures (24). It is found that mammalian glycosyltransferases are relatively hard to express in large quantities and are more rigid in terms of substrate specificity. In contrast, their bacterial counterparts are more easily overexpressed as soluble and active forms without complicated gene manipulation techniques. Furthermore, bacterial glycosyltransferases seem to have broader acceptor–substrate specificities, thereby offering tremendous advantages in the enzymatic synthesis of oligosaccharides and their analogues. In addition, various bacteria exhibit structural mimicry of mammalian glycocon-



jugates on their cell surface as a survival and infection strategy. Therefore, the corresponding glycosyltransferases might be explored for the *in vitro* synthesis of various glycoconjugates. In fact, a number of bacterial glycosyltransferases have been successfully applied in the synthesis of oligosaccharide moieties of various glycolipids, such as gangliosides (25), blood group antigens (22), and globo-series glycosphingolipids (13, 25–27).

T-Antigen has been recognized as an important tumor antigen that is exploited for the clinical development of carbohydrate-based anticancer vaccines. Various chemical strategies have been developed to synthesize T-antigen-containing glycopeptides (28). On the other hand, several eukaryotic glycosyltransferases have been identified to make T-antigens in different species. Ju et al. (29) cloned and identified a human core-1  $\beta$ 1,3-galactosyltransferase and showed that the enzyme can generate the core-1 structure from a synthetic glycopeptide with GalNAc linked to a Thr residue. Subsequently, a rat core-1  $\beta$ 1,3-galactosyltransferase was cloned (30), characterized, and shown to glycosylate GalNAc- $\alpha$ -O-Ph to provide T-antigen mimicry. More recently, the corresponding enzymes in *Drosophila* and *C. elegans* (31, 32) were also reported. Several bacterial  $\beta$ 1,3-galactosyltransferases have also been studied, all of which have endogenous acceptor specificity, different from the GalNAc $\alpha$  structure present in the T-antigen. We previously reported identification of a  $\beta$ 1,3-galactosyltransferase, WbnJ, involved in the *E. coli* O86 O-polysaccharide biosynthesis and showed that WbnJ could synthesize a T-antigen analogue (22). However, the detailed biochemical and substrate specificity study has not been carried out. Nonetheless, it was to our knowledge the first bacterial glycosyltransferase to make a T-antigen structure. In our current study, we characterized a second  $\beta$ 1,3-galactosyltransferase WbiP from *E. coli* O127. A detailed substrate specificity study showed that WbiP can be used for the facile synthesis of a variety of T-antigen mimics.

Most of the glycosyltransferases in the GTA family possess one or more DXD motifs, which have been shown to be involved in the coordination of a divalent metal ion that is required for the binding of sugar nucleotides in the active site (33, 34). Thus, characterization of the DXD motif is an important step to understanding glycosyltransferase mechanisms. Recently, both structural and biochemical studies revealed that if more than one DXD motif is present, not all the DXD motifs are functionally equivalent. A study (35) in the analysis of two DXD motifs in human xylosyltransferase I showed that the  $^{314}\text{DED}^{316}$  motif did not participate in catalysis, while the  $^{745}\text{DWD}^{747}$  motif was clearly involved in the binding of the sugar nucleotide. A well studied galactosyltransferase LgtC from *Neisseria meningitidis* contains four DXD motifs (36). The crystal structure of LgtC revealed that only two DXD motifs were located within the active site. However, of these two, one of them indeed acts to coordinate the  $\text{Mn}^{2+}$  ion with the phosphate group of UDP, whereas the other is involved in the binding of the sugar acceptor. In our study, WbiP possesses two DXD motifs,  $^{88}\text{DSD}^{90}$  and  $^{174}\text{DYD}^{176}$ . Mutation studies on these two motifs indicated that they may play different roles in enzyme catalysis. Mutation of aspartic acid into alanine at the  $^{88}\text{DSD}^{90}$  position completely abolished the enzyme activity, while marginal activity was still retained with the same mutations at  $^{174}\text{DYD}^{176}$  position, suggesting

that  $^{88}\text{DSD}^{90}$  is more essential and may directly involve in the binding of sugar nucleotides in the active site. In the kinetic studies, substantially reduced affinity for sugar donor UDP-Gal was observed for mutants D88E and D90E, while the affinity for sugar acceptors was similar to the wild-type. This observation further supports the role of  $^{88}\text{DSD}^{90}$  in the coordination of UDP-Gal binding. On the other hand, similar sugar donor affinity but reduced sugar acceptor affinity were observed for the mutants of  $^{174}\text{DYD}^{176}$ , suggesting that the  $^{174}\text{DYD}^{176}$  motif may be involved in the binding of the sugar acceptor. A third biochemical study, UDP-beads binding assay, adds another piece of experimental evidence to the differential roles of these two DXD motifs, in that reduced binding efficiency was observed in  $^{88}\text{DSD}^{90}$  mutants but not in  $^{174}\text{DYD}^{176}$  mutants. It is worth noting that a number of bacterial  $\beta$ 1,3-galactosyltransferases annotated in the database appear to possess these two conserved DXD motifs, suggesting a common glycosyl transfer mechanism. The elucidation of the functional roles of these two DXD motifs requires determination of the enzyme 3-D structure.

## ACKNOWLEDGMENT

We thank Juliana Pernik for her excellent administrative assistance.

## SUPPORTING INFORMATION AVAILABLE

Sequences of primers used in site-directed mutagenesis of WbiP, donor specificity study of WbiP, and MS spectrum of 2-AB labeled product of WbiP-catalyzed reaction with GalNAc as the substrate. This material is available free of charge via the Internet at <http://pubs.acs.org>.

## REFERENCES

1. Hang, H. C., and Bertozzi, C. R. (2005) The chemistry and biology of mucin-type O-linked glycosylation, *Bioorg. Med. Chem.* 13 (17), 5021–5034.
2. Garner, B., et al. (2001) Structural elucidation of the N- and O-glycans of human apolipoprotein(a): role of o-glycans in conferring protease resistance, *J. Biol. Chem.* 276 (25), 22000–22208.
3. Ellies, L. G., et al. (2002) Sialyltransferase ST3Gal-IV operates as a dominant modifier of hemostasis by concealing asialoglycoprotein receptor ligands, *Proc. Natl. Acad. Sci. U.S.A.* 99 (15), 10042–10047.
4. Smith, K. A. (1988) Interleukin-2: inception, impact, and implications, *Science* 240 (4856), 1169–1176.
5. Altschuler, Y., et al. (2000) Clathrin-mediated endocytosis of MUC1 is modulated by its glycosylation state, *Mol. Biol. Cell* 11 (3), 819–831.
6. Primakoff, P., and Myles, G. D. (2002) Penetration, adhesion, and fusion in mammalian sperm-egg interaction, *Science* 296 (5576), 2183–2185.
7. Hooper, L. V., and Gordon, J. I. (2001) Commensal host-bacterial relationships in the gut, *Science* 292 (5519), 1115–1118.
8. Brockhausen, I. (1999) Pathways of O-glycan biosynthesis in cancer cells, *Biochim. Biophys. Acta* 1473 (1), 67–95.
9. Sotiriadis, J., et al. (2004) Thomsen-Friedenreich (T) antigen expression increases sensitivity of natural killer cell lysis of cancer cells, *Int. J. Cancer* 111 (3), 388–397.
10. Springer, G. F. (1997) Immunoreactive T and Tn epitopes in cancer diagnosis, prognosis, and immunotherapy, *J. Mol. Med.* 75 (8), 594–602.
11. Coon, J. S., Weinstein, R. S., and Summers, J. L. (1982) Blood group precursor T-antigen expression in human urinary bladder carcinoma, *Am. J. Clin. Pathol.* 77 (6), 692–699.
12. Laurent, J. C., Noel, P., and Faucon, M. (1978) Expression of a cryptic cell surface antigen in primary cell cultures from human breast cancer, *Biomedicine* 29 (8), 260–261.

13. Shao, J., et al. (2002) Overexpression and biochemical characterization of beta-1,3-N-acetylgalactosaminyltransferase LgtD from *Haemophilus influenzae* strain Rd, *Biochem. Biophys. Res. Commun.* 295 (1), 1–8.
14. Gilbert, M., et al. (2000) Biosynthesis of ganglioside mimics in *Campylobacter jejuni* OH4384. Identification of the glycosyltransferase genes, enzymatic synthesis of model compounds, and characterization of nanomole amounts by 600-MHz H and C NMR analysis, *J. Biol. Chem.* 275 (6), 3896–3906.
15. Wang, G., et al. (1999) Novel *Helicobacter pylori* alpha 1,2-fucosyltransferase, a key enzyme in the synthesis of Lewis antigens. *Microbiology (Reading, U.K.)* 145 (11), 3245–3253.
16. Ge, Z., et al. (1997) Cloning and heterologous expression of an alpha 1,3-fucosyltransferase gene from the gastric pathogen *Helicobacter pylori*, *J. Biol. Chem.* 272 (34), 21357–21363.
17. Chan, N. W. C., et al. (1995) The biosynthesis of Lewis X in *Helicobacter pylori*, *Glycobiology* 5 (7), 683–688.
18. Rivas, M., et al. (2000) Intestinal bleeding and occlusion associated with Shiga toxin-producing *Escherichia coli* O127:H21. *Instituto Nacional de Enfermedades Infecciosas, An. Dr. Carlos G. Malbran, Buenos Aires, Argentina*, 249–252.
19. Barua, D. (1962) An outbreak of infantile diarrhoea due to *Escherichia coli* O127:B8, *Indian J. Med. Res.* 50, 612.
20. Stulberg, C. S., et al. (1955) *Escherichia coli* O127:B8, a pathogenic strain causing infantile diarrhea. I. Epidemiology and bacteriology of a prolonged outbreak in a premature nursery, *Am. J. Dis. Child.* 90 (2), 125–134.
21. Widmalm, G., and Leontin, K. (1993) Structural studies of the *Escherichia coli* O127 O-antigen polysaccharide, *Carbohydr. Res.* 247, 255–262.
22. Yi, W., et al. (2005) *Escherichia coli* O86 O-antigen biosynthetic gene cluster and stepwise enzymatic synthesis of human blood group B antigen tetrasaccharide, *J. Am. Chem. Soc.* 127 (7), 2040–2041.
23. Feizi, T., and Bundle, D. (1994) Carbohydrates and glycoconjugates. Editorial overview, *Curr. Opin. Struct. Biol.* 4 (5), 673–676.
24. Blixt, O., and Razi, N. (2006) Chemoenzymatic synthesis of glycan libraries, *Methods Enzymol* 415, 137–153.
25. Antoine, T., et al. (2003) Large-scale in vivo synthesis of the carbohydrate moieties of gangliosides GM1 and GM2 by metabolically engineered *Escherichia coli*, *ChemBioChem* 4 (5), 406–412.
26. Chen, X., et al. (2002) Reassembled biosynthetic pathway for large-scale carbohydrate synthesis: alpha-gal epitope producing “superbug”, *ChemBioChem* 3 (1), 47–53.
27. Randrianisoa, M., et al. (2007) Synthesis of globopentose using a novel beta 1,3-galactosyltransferase activity of the *Haemophilus influenzae* beta 1,3-N-acetylgalactosaminyltransferase LgtD, *FEBS Lett.* 581 (14), 2652–2656.
28. Brocke, C., and Kunz, H. (2002) Synthesis of tumor-associated glycopeptide antigens, *Bioorg. Med. Chem.* 10 (10), 3085–3112.
29. Ju, T., et al. (2002) Cloning and expression of human core 1 beta 1,3-galactosyltransferase, *J. Biol. Chem.* 277 (1), 178–186.
30. Ju, T., Cummings, R. D., and Canfield, W. M. (2002) Purification, characterization, and subunit structure of rat core 1 beta 1,3-galactosyltransferase, *J. Biol. Chem.* 277 (1), 169–177.
31. Ju, T., Zheng, Q., and Cummings, R. D. (2006) Identification of core 1 O-glycan T-synthase from *Caenorhabditis elegans*, *Glycobiology* 16 (10), 947–958.
32. Muller, R., et al. (2005) Characterization of mucin-type core-1 beta 1–3 galactosyltransferase homologous enzymes in *Drosophila melanogaster*, *FEBS J.* 272 (17), 4295–4305.
33. Davies, G. J., Gloster, T. M., and Henrissat, B. (2005) Recent structural insights into the expanding world of carbohydrate-active enzymes, *Curr. Opin. Struct. Biol.* 15 (6), 637–645.
34. Schuman, B., Alfaro, J. A., and Evans, S. V. (2007) Glycosyltransferase structure and function, *Top. Curr. Chem.* 272 (Bioactive Conformation I), 217–257.
35. Goetting, C., et al. (2004) Analysis of the DXD Motifs in Human Xylosyltransferase I Required for Enzyme Activity, *J. Biol. Chem.* 279 (41), 42566–42573.
36. Persson, K., et al. (2001) Crystal structure of the retaining galactosyltransferase LgtC from *Neisseria meningitidis* in complex with donor and acceptor sugar analogs, *Nat. Struct. Biol.* 8 (2), 166–175.

BI7020712